LA-UR-00-2789
Approved for public release; distribution is unlimited.

Title: **Beam Diagnostic Instrumentation for the Low–Energy Demonstration Accelerator (LEDA): Commissioning and Operational Experience**

Author(s): J. D. Gilpatrick, D. Barr, L. Day, K. Kasemir, W. Lysenko, M. Pieck, J.F. Power, W. Sellyey, R. B. Shurter, M. Stettler, Los Alamos National Laboratory, Los Alamos, NM, USA
J. Kamperschroer, D. Martinez, General Atomics, San Diego, CA, USA
J. O'Hara, Honeywell, Albuquerque, NM, USA
D. Madsen, ARES Corporation, Los Alamos, NM, USA

Submitted to:

http://lib-www.lanl.gov/cgi-bin/getfile?00818835.pdf

Beam Diagnostic Instrumentation for the Low–Energy Demonstration Accelerator (LEDA): Commissioning and Operational Experience

J. D. Gilpatrick, D. Barr, L. Day, K. Kasemir, W. Lysenko, M. Pieck, J.F. Power, W. Sellyey, R. B. Shurter, M. Stettler, Los Alamos National Laboratory, Los Alamos, NM, USA
J. Kamperschroer, D. Martinez, General Atomics, San Diego, CA, USA
J. O'Hara, Honeywell, Albuquerque, NM, USA
D. Madsen, ARES Corporation, Los Alamos, NM, USA

Abstract

The LEDA facility has been used to characterize the pulsed- and cw-beam performance of a 6.7-MeV, 100-mA radio frequency quadrupole (RFQ). Diagnostic instrumentation, primarily located in a short beam transport downstream of the RFQ, allowed facility commissioners and operators to measure and monitor the RFQ's accelerated and total beam transmission, beam loss, bunched beam current, beam energy and output phase, and beam position. Transverse beam profile measurements are acquired under both low and high duty-factor pulsed beam conditions using a slow wire scanner and a camera that images beam-induced fluorescence. The wire scanner is also used to acquire transverse beam emittance information using a technique known as a "quad scan". This paper reviews the measurement performance and discusses some of the resulting data.

1 INSTRUMENTED BEAM TRANSPORT

The primary purpose of the high-energy beam transport (HEBT) is to safely transport the nominally 6.7-MeV, 100-mA beam from the exit of the RFQ to a 670-kW beam stop [1,2,3]. The HEBT also serves as a platform for beam instrumentation that enabled the accelerator commissioners and operators to characterize the RFQ output beam and to monitor the beam during both pulsed and cw beam operation [4]. This particular HEBT uses four quadrupole magnets to transport and expand the beam on the beam stop and to limit the beam's peak and average power density. Two steering magnets keep the beam centered throughout the HEBT. In addition, a pulsed (or ac) toroid was placed at the RFQ entrance so that beam transmission could be monitored during pulsed beam operation. There is additional instrumentation located in the H^+ injector that is not discussed here.

2 BEAM TRANSMISSION

There are three types of beam current measurements: dc, pulsed (or ac), and bunched beam current. Using ac toroids at the entrance and exit of the RFQ and HEBT, RFQ and HEBT beam transmission data are acquired during all phases of the RFQ operation [3,4]. Cw beam transmission was obtained in similar fashion using Bergoz™ DCCTs. If the RFQ accelerating fields are set at or near their design level, most particles caught within the rf bucket are both accelerated to the nominal beam energy and bunched at the RFQ 350-MHz resonant frequency. To measure accelerated beam transmission, the RFQ output bunched beam current is compared to the total input pulsed or cw beam current. Fig. 1 plots the measured total and accelerated RFQ transmission and the measured HEBT total beam transmission as a function of the RFQ accelerating field level.

Early in the RFQ operation, both the RFQ cw and pulsed beam transmission measurements displayed transmission efficiencies of greater than 100%, clearly indicating a faulty measurement. The suspected cause of this faulty condition was forward-scattered electrons passing through the RFQ entrance toroid. The measurement error was corrected by the addition of an electron trap in the RFQ entrance end wall. The ring-shaped trap's primary purpose was to maintain the background neutralization gas pressure in the beam region near the RFQ entrance so that the beam's convergence angle could be optimized [5]. However, an additional benefit of disallowing forward streaming electrons resulted in an accurate pulsed-beam RFQ transmission measurement (i.e., transmission accuracy typically 1%).

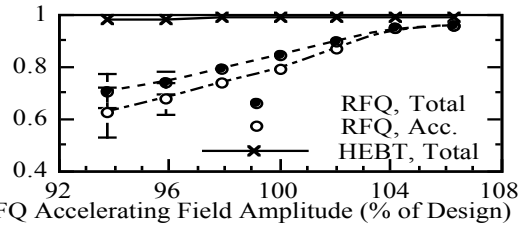

Figure 1: RFQ total and accelerated beam transmission and HEBT total beam transmission are plotted. Vertical error bars describe the transmission variations due to time-dependent beam current variations.

Due to the ionizing radiation levels in the beam line near the DCCTs, the supplied analog electronics were installed outside the beam tunnel. This decision resulted in the addition of approximately 50 m of a cable between

This work supported by the US Department of Energy.

the multi-core toroidal DCCT and its associated electronics.

3 BEAM LOSS

There are two types of beam loss measurements: a differential current measurement using two sequential toroidal transformers, and the measurement of the ionizing radiation using both ionization chambers and proportional counters. Within each pulsed-current monitor's processor resides a digital-signal-processor (DSP). This DSP applies an in-situ calibrator correction to the current measurement signal on every 2-μs digitized sample [6,7]. These sampled signals are then digitally integrated and compared to a predefined lost beam-charge condition. If too much lost charge is detected, as defined by the operator screen input, a digital logic signal line instructs the fast protection system to shut off the injected beam. This differential lost-current VXI-module hardware performed reliably even with occasional crate controller and Ethernet faults.

Ionization chambers detect prompt ionizing radiation resulting from the interaction between the proton beam and beam line components [8]. For 6.7-MeV protons, the amount of ionizing radiation is typically less than what much higher energy beams would produce. To verify that the ionization chambers were sufficiently sensitive to lost beam currents of less than 0.25 mA, a test was configured using the slow wire scanner. The results showed that the ionization chambers could detect 0.1 mA of lost beam. Of course, this precision will be different for protons on a stainless steel beam pipe.

4 BEAM ENERGY AND PHASE

Three capacitive probes and a B-dot RFQ field probe provided the rf signals to measure the beam central energy and phase [9,10]. A time-of-flight technique is used to measure beam energy employing two capacitive probes separated by a known distance and differential phase measurement electronics. The output phase is measured by detecting the phase difference between the first HEBT capacitive probe and the RFQ B-dot field probe, and subtracting off the phase errors due to changes in beam energy.

5 TRANSVERSE BEAM PROFILES

The LEDA HEBT has two acquisition methods for transverse beam distributions: a slow wire scanner (WS) during low duty-factor pulsed-beam, and a background gas fluorescence technique during high duty factor or cw beam operation. Both measurements are physically mounted on the HEBT such that they can view the same beam region.

The WS's primary purpose is to verify that the beam width is sufficiently expanded under low duty-factor pulsed conditions to guarantee beam stop safety under cw beam operational conditions [11]. The beam size was determined by first comparing the beam's rms width with the expected size as predicted by the envelope transport code, TRACE 3-D [12]. The beam expansion "rate" was inferred by changing the final quadrupole magnet's fields and calculating the rate expansion from the beam width changes.

With the proper transport quadrupole magnet fields and associated profile data, a technique commonly known as a "quad scan" can be performed to determine the beam's rms emittance and associated Courant-Snyder parameters. This technique was used to characterize the RFQ output beam by acquiring a series of transverse profiles for various upstream quadrupole field levels. For example, as the magnet field is reduced in the quadrupole magnet nearest the RFQ exit, a waist in the vertical plane can be moved through the WS plane. The resulting beam profile data can then be fit to the model of the expected beam trajectory as predicted by TRACE 3-D. Typically, this technique has been used with beams that have relatively low space charge forces such that the fit model could be approximated with a quadratic equation. However, the LEDA beam has high space charge forces, i.e., rms widths of 1- to 2-mm and a beam current of 100-mA, so the simple models will not accurately reflect the beam behavior. A new application of the quad scan technique presently being explored is the utilization of particle simulation codes with the appropriate space charge subroutines included as the fit model. A paper to be presented in the upcoming LINAC2000 conference will provide further details of this technique [13].

Experiments were conducted to understand the limits of the WS 0.1-mm SiC-coated carbon fiber [11]. WS fiber was inserted into the proton beam core. Starting with a short macropulse, the macropulse length was extended until the fiber's emitted electron current was nonlinear with time. Fig. 2 shows the emitted electron current as a function of macropulse length. The secondary-electron (S.E.) emission region is modeled by the linear flat portion of the data to 1.2 ms, and therefore, independent of time and temperature. The S.E. emission current during this initial 1.2-ms portion of the data was approximately 9 μA, resulting in a S.E. coefficient of 3.3 %. The nonlinear thermionic emission (T.E.) region later in the macropulse is modeled by a second-order polynomial – the Richardson-Dushman equation that describes T.E. emission has a temperature-squared term. While acquiring the emission data, optical spectra were also acquired. The beam/fiber thermal model that fits the spectrum data (i.e., radiative cooling only) do not completely agree with the electron emission data but they likely bracket the temperature at which the emission data transistions between S.E. and T.E. emission. Substituting this temperature range of 1575 K to 2050 K into the Richardson-Dushman equation, the work function for this particular SiC fiber was calculated to be between 2.4- and 3.2-eV.

The background gas fluorescence technique has been used to acquire high peak current beam profile

measurements. As protons in the ion beam pass near background gas molecules, some of the protons excite the molecules' electrons to higher energy levels. There is some debate whether the resulting electron transition back to the ground state is either a molecular or atomic process, but in either case, fast single transitions produce fluorescence spectral lines. The two primary lines are at 391- and 426-nm. If the lines are atomic, their lifetimes are approximately 0.2- and 0.1-μs, respectively, and can be shown to be very short with respect to the transit times of the gas molecules [14].

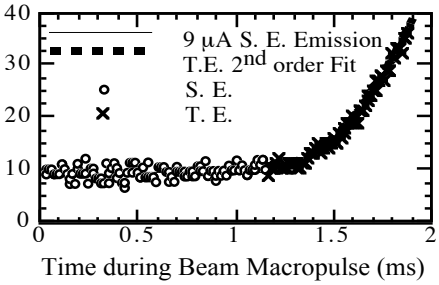

Figure 2. As beam intercepts the SiC-coated carbon fiber, the fiber emits secondary and thermionic electrons (S. E. and T.E. respectively). Thermionic electrons dominate the electron emission 1.2 ms into the macropulse.

6 BEAM POSITION

The beam position measurements consist of a traditional micro-stripline beam position monitor (BPM) whose downstream port is terminated in its 50-Ω characteristic impedance [15]. The electronics log-ratio processor is integrated with the EPICS control system interface, all within the VXI module [16]. The processor module has a built-in calibration and test function that verifies the system operation and an error-correcting calibration procedure that removes errors due to additional cable attenuation and log function non-conformity.

The heart of the log-ratio processor is the Analog Devices AD8307 logarithmic detector/amplifier [17,18]. This log amplifier uses the successive approximation technique to approximate the true logarithmic function. To further reduce these errors, an injected signal is swept through the full dynamic range and a correction table is generated for each of the four independent BPM-electrode channels. This error is then subtracted from each electrode at every 1-μs sample. The resulting accuracy of each log ratio processor axis is typically less than +/-0.1 dB over greater than a 45-dB dynamic range.

REFERENCES

[1] J. D. Gilpatrick, et al., "Low Energy Demonstration Accelerator (LEDA) Beam Instrumentation: RFQ-Accelerated Beam Results", PAC'99, New York City, NY, March 29, 1999, pp. 2214-2216.

[2] J. D. Schneider, et al., "Overview of High-Power CW Proton Accelerators", these proceedings.

[3] H. V. Smith, et al., "Commissioning Results from the Low-Energy Demonstration accelerator (LEDA) Radio-Frequency Quadrupole (RFQ)", these proceedings.

[4] J. D. Gilpatrick, et al., "LEDA Beam Diagnostics Instrumentation: Measurement Comparisons and Operational Experience", BIW '00, Boston, MA, May 8-11, 2000.

[5] L. M. Young, et al., "High Power Operation of LEDA", to be published in upcoming LINAC2000 Conference, Monterey, CA, August, 21-25, 2000.

[6] D. Barr, et al., "LEDA Beam Diagnostics Instrumentation: Beam Current Measurement", BIW '00, Boston, MA, May 8-11, 2000.

[7] J. F. Power, et al., "Beam Current Measurements for LEDA", PAC'99, New York City, NY, May, 1999, pp. 2241-2243.

[8] W. Sellyey, et al., "Experience With Beam Loss Monitors In The Low Energy Demonstration Accelerator (LEDA)", BIW '00, Boston, MA, May 8-11, 2000.

[9] J. F. Power, et al., "Performance of the Beam Phase Measurement System for LEDA", BIW '00, Boston, MA, May 8-11, 2000.

[10] J. D. Gilpatrick, et al., "Experience with the Ground Test Accelerator Beam Measurement Instrumentation", in AIP Conference Proceedings 319, Santa Fe, NM, August, 1993, p. 154.

[11] J. O'Hara, et al., "Slow Wire Scanner Beam Profile Measurement for LEDA", BIW '00, Boston, MA, May 8-11, 2000.

[12] TRACE 3-D is a beam envelope simulation code supported by the LANL Code Group.

[13] W. Lysenko, et al., "Determining Phase-Space Properties of the LEDA RFQ Output Beam", to be published in upcoming LINAC2000 Conference, Monterey, CA, August, 21-25, 2000.

[14] J. Kamperschroer, "Initial Operation of the LEDA Beam-Induced Fluorescence Diagnostic", BIW '00, Boston, MA, May 8-11, 2000.

[15] J. D. Gilpatrick, "LEDA and APT Beam Position Measurement System: Design and Initial Tests", LINAC'98, August, 1998, pp. 532-534.

[16] D. Barr, et al., "LEDA Beam Diagnostics Instrumentation: Beam Position Monitors," BIW '00, Boston, MA, May 8-11, 2000.

[17] J. D. Gilpatrick, "Comparison Of Beam-Position-Transfer Functions Using Circular Beam-Position Monitors", PAC'97, Vancouver, BC, Canada, May, 1997, pp. 2090-2092.

[18] R. B. Shurter, et al., "BPM Analog Front End Electronics Based on the AD8307 Log Amplifier", BIW '00, Boston, MA, May 8-11, 2000.